Properties of the second outburst of the bursting pulsar (GRO J1744-28) as observed with BATSE

Woods, P.M.; Kouveliotou, C.; van Paradijs, J.A.; Briggs, M.S.; Wilson, C.A.; Deal, K.; Harmon, B.A.; Fishman, G.J.; Lewin, W.H.G.; Kommers, J.

Published in:
Astrophysical Journal

DOI:
10.1086/307171

THE ASTROPHYSICAL JOURNAL, 517:431–435, 1999 May 20

PROPERTIES OF THE SECOND OUTBURST OF THE BURSTING PULSAR (GRO J1744−28) AS OBSERVED WITH BATSE

PETER M. WOODS,[1] CHRYSSA KOUVELIOTOU,[2,3] JAN VAN PARADIJS,[1,4] MICHAEL S. BRIGGS,[1] C. A. WILSON,[3] KIM DEAL,[1] B. A. HARMON,[3] G. J. FISHMAN,[3] W. H. G. LEWIN,[5] AND J. KOMMERS[5]

Received 1998 June 5; accepted 1998 December 28

ABSTRACT

One year after its discovery, the Bursting Pulsar (GRO J1744−28) went into outburst again, displaying the hard X-ray bursts and pulsations that make this source unique. We report on BATSE observations of both the persistent and burst emission for this second outburst and draw comparisons with the first. The second outburst was smaller than the first in both duration and peak luminosity. The persistent flux, burst peak flux, and burst fluence were all reduced in amplitude by a factor of ∼1.7. Despite these differences, the two outbursts were very similar with respect to the burst occurrence rate, the durations and spectra of bursts, the absence of spectral evolution during bursts, and the evolution of the ratio α of average persistent to burst luminosity. Although no spectral evolution was found within individual bursts, we find evidence for a small (20%) variation of the spectral temperature during the course of the second outburst.

Subject headings: pulsars: individual (GRO J1744−28) — X-rays: bursts — X-rays: stars

1. INTRODUCTION

The Bursting Pulsar was initially detected as an X-ray burster (Fishman et al. 1995; Kouveliotou et al. 1996b) on 1995 December 2 when a series of hard X-ray bursts separated by ∼3 minutes was detected with the Burst and Transient Source Experiment (BATSE) on board the *Compton Gamma-Ray Observatory*. One month later a persistent source, GRO J1744−28, was also discovered with BATSE (Paciesas et al. 1996) from the same general direction near the Galactic center. Soon after, it was realized that GRO J1744−28 is a 467 ms pulsar in a binary system with an 11.8 day orbital period and a mass function of $1.36 \times 10^{-4}\ M_{\odot}$ (Finger et al. 1996a, 1996b). These parameters indicated that the companion is a low-mass star, and the system was consequently classified as a low-mass X-ray binary. During early January 1996 the 467 ms pulsations were also found during the bursts at an enhanced amplitude (Kouveliotou et al. 1996a), which led to the conclusion that the burster and the pulsar are the same source, hence the name "Bursting Pulsar."

The source remained active for the next 1.5 yr, showing two major outbursts. The first lasted until 1996 May 3, when bursting activity temporarily ceased. For the next 7 months, the persistent flux remained variable but at a lower level relative to the major outbursts (Kouveliotou & van Paradijs 1997; Stark et al. 1997). Also during this time, intermittent weak burst activity was observed (Cui 1997) with the Proportional Counter Array (PCA) on board the *Rossi X-Ray Timing Explorer* (*RXTE*). The second outburst began on 1996 December 1 and lasted through ∼1997 April 7. From the end of the second outburst until 1998 October, no activity from this source was detected by either BATSE or *RXTE*.

During the course of these outbursts, BATSE observed more than 5800 X-ray bursts from the Bursting Pulsar that at times reached peak luminosities of $L \sim 100 L_{\rm Edd}$ (Jahoda et al. 1997). These bursts are almost certainly type II bursts due to spasmodic accretion onto the surface of a neutron star, similar to those seen from the rapid burster (Kouveliotou et al. 1996b; Lewin et al. 1996; Kommers et al. 1997). Cannizzo (1996) has proposed a particular model that describes the nature of the accretion instability leading to the X-ray burst. An alternative burst emission mechanism involving thermonuclear burning on a neutron star has been considered by Bildsten & Brown (1997) and Lamb, Miller, & Taam (1996).

Here we discuss the second outburst, during which BATSE detected 2709 bursts from the Bursting Pulsar. We describe the properties of these bursts and their relation to the persistent emission and make comparisons with the first outburst. A more detailed account of the BATSE results for the first outburst can be found in Kouveliotou & van Paradijs (1997) and Briggs et al. (1999). A comparison of the properties of the pulsations during bursts as observed in the two outbursts will be presented by Woods et al. (1999).

2. TEMPORAL PROPERTIES

One year after its discovery, the Bursting Pulsar went into outburst for the second time. Similar to the first outburst, the second outburst started with a very high burst rate during the first 24 hr. However, the peak fluxes of these early bursts of the second outburst were weaker by a factor of ∼1.4. This placed the average peak flux value near the BATSE sensitivity threshold, thereby making identification of these events rather difficult. This resulted in a larger uncertainty for the burst occurrence rate near the beginning and end of the outburst. Even with an increased uncertainty, the burst rate of the first 24 hr of ∼135 bursts per day, corrected for exposure time, is significantly larger than the average rate through the remainder of the outburst, which is about 20 events per day observed (∼35–40 events per day corrected for exposure; see Fig. 1). This rate remained fairly constant over the next 4 months despite a net variation in the average burst peak flux by a factor of

[1] Department of Physics, University of Alabama in Huntsville, Huntsville, AL 35899.
[2] Universities Space Research Association.
[3] NASA Marshall Space Flight Center, ES–84, Huntsville, AL 35812.
[4] Astronomical Institute "Anton Pannekoek," University of Amsterdam, 403 Kruislaan, 1098 SJ Amsterdam, Netherlands.
[5] Department of Physics and Center for Space Research, Massachusetts Institute of Technology, Cambridge, MA 02138.

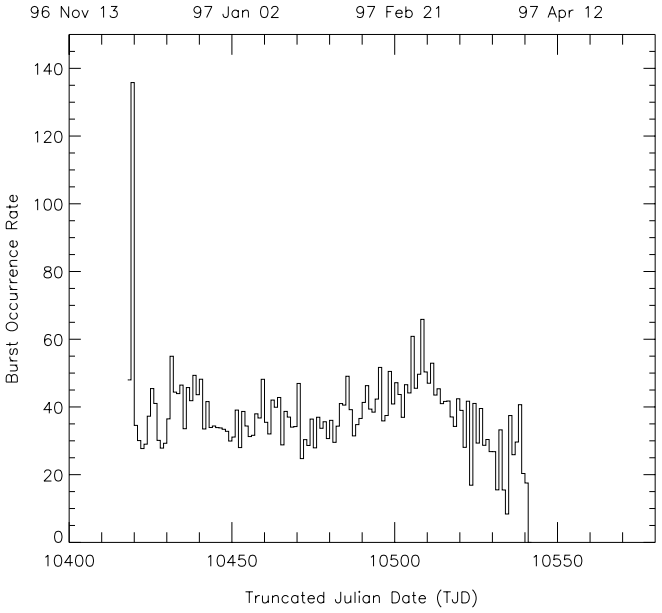

FIG. 1.—Daily burst occurrence rate corrected for exposure time. Truncated Julian Date (TJD) = Julian Date − 2440000.5.

~5. Bursts were observed with BATSE until 1997 April 2, when the burst fluxes dropped below the BATSE sensitivity level. We calculated for all detected events: the rise times, decay times, and durations using the 1.024 s time-resolution data (DISCLA data type) in the energy range ~25–50 keV.

From observations of the time profiles of thousands of these events, it appears that the burst shape does not change much through the outburst. On the 1.024 s timescale, the bursts show one maximum with varying rise and decay times. In order to quantify the burst durations, we fitted a two-sided Gaussian function superposed on a second-order polynomial to each event. We defined this function to be two half-Gaussian functions with the same value of the peak, mean, and underlying polynomial but different widths in order to account for the varying rise and decay times. We

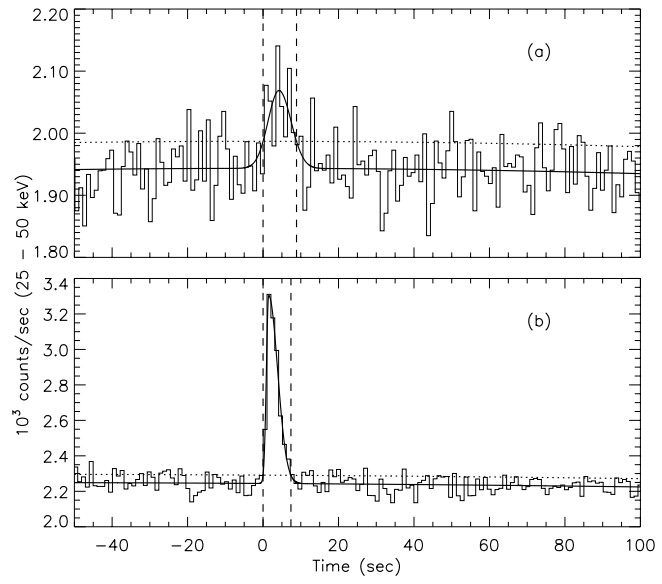

FIG. 2.—Examples of duration measurements for two bursts from (*a*) TJD 10434 (1996 December 17) and (*b*) TJD 10472 (1997 January 24).

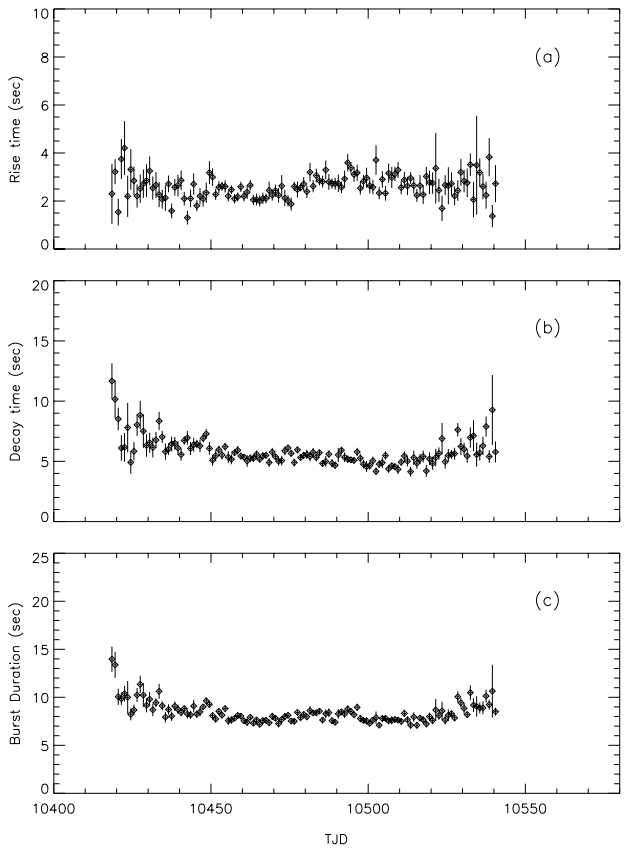

FIG. 3.—Daily mean rise times (*a*), decay times (*b*), and burst durations (*c*). The error bars represent sample variance.

show two examples in Figures 2*a* and 2*b*. The histogram represents the data, while the continuous bold line represents the fit. The dotted line denotes the 1 σ level above the fitted background. We chose the intersection points of the fit with the 1 σ background level to define the start and end times of each burst (*vertical dashed lines*). The differences between these times and the peak of the two Gaussian functions are defined as the rise and decay times, respectively. We calculated durations (differences between start and end times, i.e., rise time plus decay time) for 2385 of the 2709 bursts. Telemetry data gaps, inadequate fits (usually for weak bursts), or severely changing background levels were the main reasons for excluding 324 bursts. We find a mean rise time of 2.6 ($\sigma_{\rm rise} = 0.5$ s) and decay time of 5.8 s ($\sigma_{\rm decay} = 1.2$ s). Figure 3 displays the rise time (Fig. 3*a*), decay time (Fig. 3*b*), and total duration (Fig. 3*c*) of these events averaged for each day through the outburst. After the initial flurry of relatively longer bursts (~15 s durations) at the onset of the outburst, we find that the subsequent burst durations show little variation (range ~7–11, mean duration = 8.2, $\sigma_{\rm duration} = 2.0$ s). Some of this variation is probably due to systematic effects introduced by our estimation of the burst profile as purely Gaussian.

3. SPECTRAL PROPERTIES

To analyze the spectra of bursts, we used data that are accumulated with a 2.048 s time resolution over 16 energy channels covering the range of ~25 keV to greater than 1 MeV (CONT data type). For a complete description of the various data types of BATSE, see Fishman et al. (1989). The background was estimated by fitting a polynomial of order

no greater than 4 to about 300 s of preburst and postburst data for each burst. The background-subtracted burst spectra were then fitted to a simple, optically thin thermal bremsstrahlung (OTTB) model for the energy range 30–100 keV, where the photon flux is given by

$$\frac{dN}{dE} \propto \frac{1}{E} \exp\left[-\left(\frac{E}{kT}\right)\right]. \quad (1)$$

Data gaps and background modeling limited the number of fits to 2472 bursts for this analysis. Fitting these events individually, we were able to determine the temperature, kT, only for the more intense events (38%). These spectral fits returned reasonable reduced χ^2 values with a mean value of ~ 1.4. In order to estimate kT for the remainder, it was necessary to fit multiple burst spectra simultaneously. We combined 20 consecutive events at a time to construct a history of the burst kT through the outburst (Fig. 4). The kT remains approximately constant at ~ 9.7 keV, with the exception of a ~ 17 day period, when it dropped to ~ 7.5 keV. A number of possible systematic effects were considered as a cause for the observed drop in burst temperature. We searched for differences in detector sets used for spectral analysis, spacecraft orientation changes, and changes with the energy mapping of the CONT data type. We find no evidence for a correlation between changes of these parameters and the burst temperature.

Using these kT measurements, we were then able to calculate the burst fluence (i.e., time-integrated flux) over the energy range 30–100 keV for all 2472 events. We find that the burst fluence ($E_{\rm burst}$) changed by a factor of ~ 4 (between 1 and 4×10^{-7} ergs cm^{-2}; Fig. 5*a*). Because of the coarse time resolution of CONT data and the relatively short bursts, we were concerned that a peak flux measurement on this timescale (2.048 s) would be systematically too small because of undersampling. To estimate the peak flux more accurately, we used another data type (DISCLA) that is accumulated with 1.024 s resolution but with coarser spectral resolution (four energy channels). We peak-aligned the bursts for each day of the outburst and integrated the total number of counts minus background during the burst interval. We then took the ratio of the average burst fluence as calculated from the CONT data to the total counts of the DISCLA data to derive conversion factors. We multiplied the peak count rate of the average burst profile by the conversion factors to estimate the peak flux (30–100 keV) on the 1.024 s timescale. We find that the peak flux ($F_{\rm burst}$) varied by a factor of ~ 5 (between 2 and 10×10^{-8} ergs cm^{-2} s^{-1}; Fig. 5*b*). The similarity in the variations of the peak flux and fluence is not surprising, since the burst duration did not change much during the outburst.

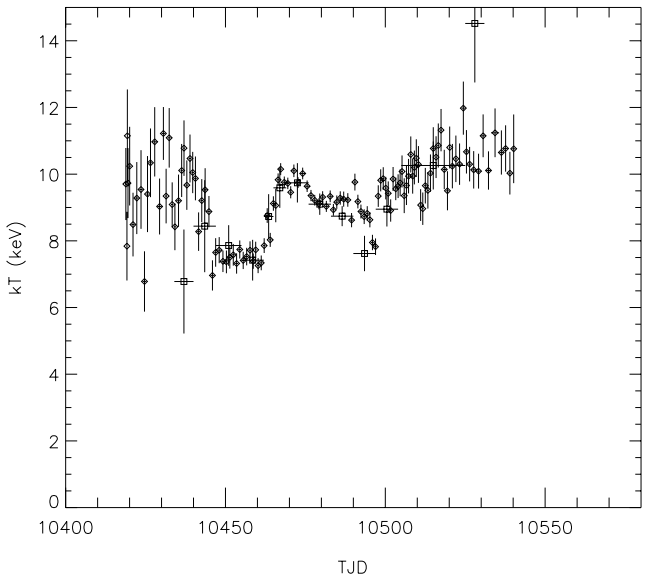

FIG. 4.—Distribution of spectral temperature, kT, as derived from the burst emission (*diamonds*) and persistent emission (*squares*).

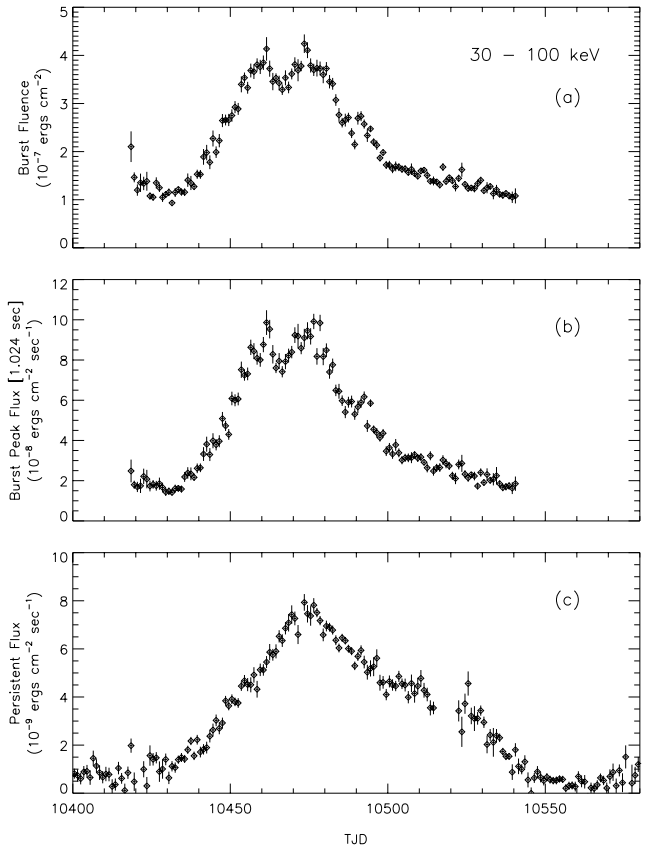

FIG. 5.—Daily averages of (*a*) burst fluence, (*b*) burst peak flux on the 1024 ms timescale, and (*c*) persistent flux (30–100 keV).

Using the Earth-occultation technique (Harmon et al. 1992), we have measured the persistent flux of GRO J1744−28 throughout its second outburst and fitted the same OTTB model used for the burst spectra to fit the persistent spectrum. It was necessary to remove a high-energy component introduced by a bright, interfering source (1E 1740.7−2942) close in angle to the Bursting Pulsar. We assumed the power-law index and energy flux to be constant at -2.5 and 2.2×10^{-9} ergs cm^{-2} s^{-1} (30–100 keV), respectively (Harmon et al. 1994). The assumption that the 1E 1740.7−2942 flux is not changing through both outbursts is supported by the *RXTE* All-Sky Monitor (ASM) quick-look results provided by the ASM/*RXTE* team, which show that 1 day averages remain relatively constant. Although the ASM is sensitive to a lower energy range (2–10 keV), this detector does not suffer as much from source confusion near the Galactic center and therefore provides a better measure of the source variability. On subtraction of the interfering component, we find that the bremsstrahlung temperature of GRO J1744−28 as derived from the persistent flux is consistent with the values

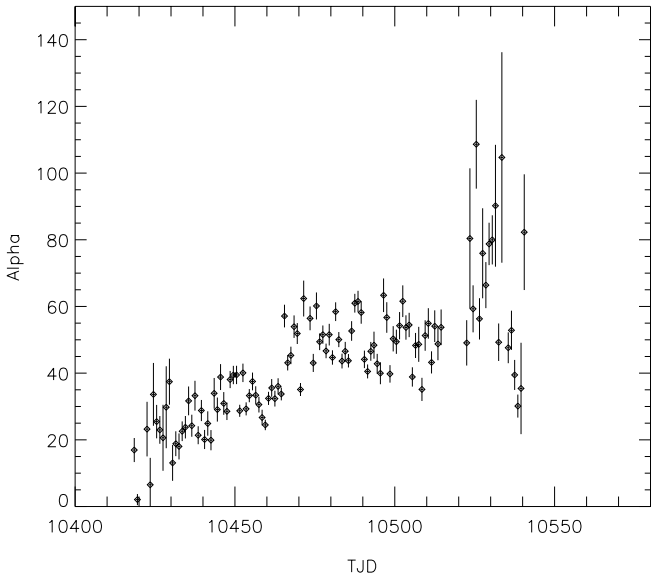

FIG. 6.—Distribution of the ratio of daily averaged persistent emission to burst emission over the energy range 30–100 keV, α.

obtained using the burst emission (Fig. 4), while the average persistent flux ($F_{\rm persis}$) varied from 1 to 8×10^{-8} ergs cm^{-2} s^{-1} (Fig. 5*c*).

Comparison of $F_{\rm burst}$ and $E_{\rm burst}$ (Figs. 5*b* and 5*a*) with $F_{\rm persis}$ (Fig. 5*c*) shows that although the overall temporal behavior of each is roughly similar, there are some differences. On the timescale of the outburst, the light curve of the persistent flux appears to be shifted relative to the light curves of the burst emission. To quantify this, we calculated the time in the outburst at which half the energy was released for both the persistent and burst emission. We found that this time for the burst emission precedes the corresponding persistent emission time by 8.1 ± 0.7 days. Also, the light curve of the persistent flux ($F_{\rm persis}$) is roughly triangular and smooth compared with the light curves of the burst emission ($F_{\rm burst}$ and $E_{\rm burst}$), which show features not seen in $F_{\rm persis}$. The single peak found in $F_{\rm persis}$ corresponds roughly with the second peak of $F_{\rm burst}$ and $E_{\rm burst}$. The prominent first peak of the burst emission that is not present in the persistent emission also overlaps with the observed drop in temperature of the bursts.

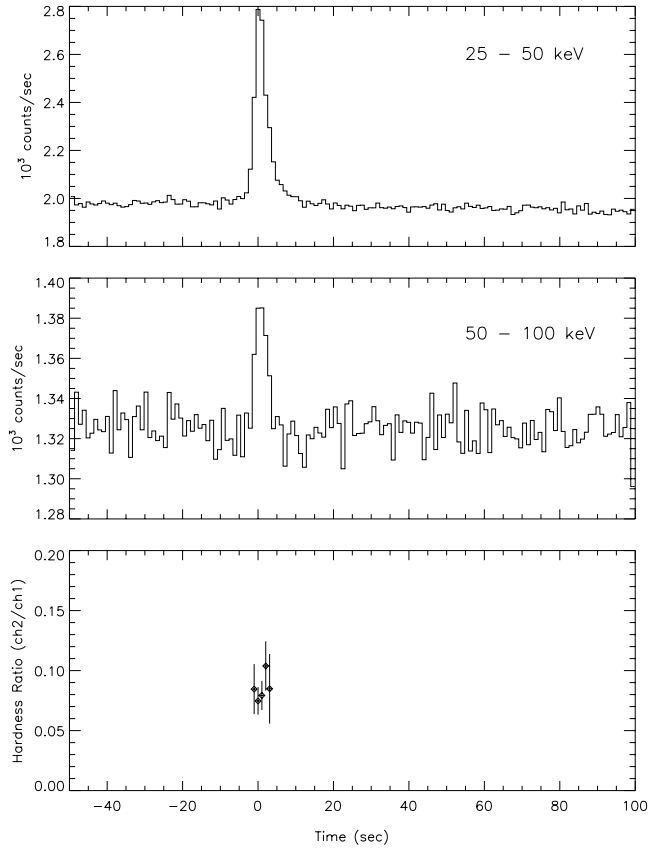

FIG. 7.—Peak-aligned average daily burst profile for TJD 10461 (1997 January 13). (*a*) 25–50 keV; (*b*) 50–100 keV; (*c*) hardness ratios during burst interval.

Combining the persistent and burst information for each day of the outburst, we calculated α, the ratio of the time-averaged bolometric persistent to burst fluxes. Since the spectral shapes of the burst and persistent emission are very similar, we can justify using a limited energy interval (30–100 keV) of the spectrum to calculate α. This is meaningful, since there is no major difference in the spectra outside the 30–100 keV energy band (Giles et al. 1996). The average persistent emission was estimated by multiplying the number of seconds in a day by the average persistent flux (Fig. 5*c*). The daily burst fluence was found by multiplying the average burst fluence (Fig. 5*a*) for each day by the burst rate (Fig. 1). The ratio of these two numbers yields α. As shown in Figure 6, α is very small at the start of the outburst ($\alpha = 2.1 \pm 1.7$ on 1996 December 2), which strongly suggests that these bursts are due to spasmodic accretion rather than thermonuclear burning (Lewin, van Paradijs, & Taam 1995). Over the next 4 months, α gradually rises to a maximum of about 80 near the end of the outburst. Since the corrected burst rate remains constant through the majority of the outburst, this rise in α is caused by the shift of the persistent flux light curve relative to the burst emission.

We also investigated the evolution of spectra *during* bursts. To accomplish this, we again used the DISCLA data type. Because of the low number of counts above 50 keV, it was necessary to align and average bursts. For each day of the outburst, bursts were peak-aligned and daily light curves created for both the 25–50 and 50–100 keV bands. The polynomial-fitted background was subtracted, and hardness ratios (i.e., the ratio of the 50–100 to the 25–50 keV counts) were calculated through the burst interval. Since we are limited by the counts available in the higher energy channel, we defined the burst interval to be the time during which the 50–100 keV count rate exceeded 2 σ above the fitted background. We then searched for changes in the hardness ratio through the average burst profile (for example, Fig. 7*c*). For each daily averaged profile, the weighted mean hardness ratio was calculated and the scatter about the mean quantified using the χ^2 statistic. Next we tested the null hypothesis (constant hardness) using the χ^2 statistic. We found that the probability of exceeding χ^2 is uniformly distributed between 0 and 1 through the outburst and never falls below 10^{-2}, indicating no evidence for spectral evolution.

4. COMPARISON WITH THE FIRST OUTBURST

The two outbursts of the Bursting Pulsar were extremely similar in many ways, even with respect to very detailed

properties. The burst-occurrence rate during the first 24 hr of each outburst was very high ($\sim$135 bursts per day on 1996 December 2 and $\sim$200 on 1995 December 2, corrected for exposure time), and the individual burst durations for these events were relatively long ($\sim$15 s). These properties resulted in a low α-value for the first 24 hr of each outburst. For both outbursts, the average burst rate and burst durations thereafter remained approximately constant at 40 bursts per day and 8 s, respectively. As in the first outburst, there is no evidence for spectral evolution within average daily burst profiles, nor do we find substantial spectral differences between the burst and persistent emission. Another common property of these outbursts is the lag of the persistent light curve relative to the burst light curves (10.1 ± 0.6 days for the first outburst in terms of difference in half-energy release times and 8.1 ± 0.7 days for the second).

The most noticeable differences between outbursts is that the second outburst was "smaller" in both duration ($\sim$20%) and persistent/burst peak intensity (by a factor of $\sim$1.7 in both). We observe moderate changes in the bremsstrahlung temperature of the burst spectra near the peak of the second outburst, in contrast to the first outburst, when the burst temperature remained relatively constant throughout the outburst. Since both the persistent and burst flux were scaled down in roughly the same way and the average burst rate did not change much between outbursts, the ratio α evolved similarly through each outburst.

Having both outbursts covered by BATSE, direct comparisons of the total energy released can also be made. Using the average burst fluence and the corrected burst rate and assuming isotropic emission, we estimated that the total energy released (30–100 keV) in burst emission during the second outburst was 7.6×10^{42} ergs (for a distance of 8 kpc), a factor of 2.1 less than the first outburst. Similarly, we find that the persistent energy released to be 3.3×10^{44} ergs, again a factor of 2.1 smaller. Integrating the persistent and burst emission over the second outburst, we find $\alpha_2 = 42.6 \pm 0.4$, the same value as found for the first outburst.

Since BATSE can only observe a fraction of the spectral range in which the source releases radiation (30–100 keV), we cannot determine the bolometric luminosity for the source directly. The PCA on board *RXTE* has an observable energy range (2–60 keV) better suited to estimate the bolometric luminosity for this source. Jahoda et al. (1997) measured the peak fluxes and fluences for a number of bursts during each outburst. Comparing the peak count rates of PCA and BATSE for bursts during the same time period, we derived a conversion factor that gives a better measure of the true bolometric energy released during the outburst. We found that the energy flux detected between 30 and 100 keV (BATSE) corresponds to roughly 5% of the energy flux within the 2–60 keV band (PCA). This implies that the total energy released (2–60 keV) during the second outburst through persistent and burst emission was $\sim 7 \times 10^{45}$ and $\sim 2 \times 10^{44}$ ergs, respectively.

We would like to thank Robert Mallozzi for help with adjusting the WINGSPAN software package for our specific applications. P. M. W. acknowledges support under grants NAG 5-3003 and NAG 5-4419 and the cooperative agreement NCC 8-65. C. K. acknowledges support under grant NAG 5-4799. J. v. P. acknowledges support under grants NAG 5-2755 and NAG 5-3674. W. H. G. L. gratefully acknowledges support from NASA.

REFERENCES

Bildsten, L., & Brown, E. F. 1997, ApJ, 477, 897
Briggs, M. S., Kouveliotou, C. K., van Paradijs, J., Woods, P., Deal, K., Lewin, W., & Kommers, J. 1999, in preparation
Cannizzo, J. K. 1996, ApJ, 466, L31
Cui, W. 1997, preprint (astro/ph-9712175)
Finger, M. H., et al. 1996a, IAU Circ. 6285
Finger, M. H., Koh, D. T., Nelson, R. W., Prince, T. A., Vaughan, B. A., & Wilson, R. B. 1996b, Nature, 381, 291
Fishman, G. J., et al. 1989, Compton Obs. Sci. Workshop, ed. W. N. Johnson (Washington, D.C.: NASA), 2
———. 1995, IAU Circ. 6272
Giles, A. B., Swank, J. H., Jahoda, K., Zhang, W., Strohmayer, T., Stark, M. J., & Morgan, E. H. 1996, ApJ, 469, L25
Harmon, B. A., et al. 1992, Compton Obs. Sci. Workshop, ed. C. R. Schrader, N. Gehrels, & B. Denis (Washington, D.C.: NASA), 69
———. 1994, in AIP Conf. Proc. 410, Proc. Fourth Compton Symp., ed. C. E. Fichtel, N. Gehrels, & J. P. Norris (New York: AIP), 456
Jahoda, K., Stark, M. J., Strohmayer, T. E., Zhang, W., Morgan, E. H., & Fox, D. 1997, preprint (astro/ph–9712340)
Kommers, J. M., Fox, D. W., Rutledge, R. E., Lewin, W. H. G., van Paradijs, J., & Kouveliotou, C. 1997, ApJ, 482, L53
Kouveliotou, C., et al. 1996a, IAU Circ. 6286
Kouveliotou, C., & van Paradijs, J. 1997, in AIP Conf. Proc. 410, Proc. Fourth Compton Symp., ed. C. D. Dermer, M. S. Strickman, & J. D. Kurfess (New York: AIP), 96
Kouveliotou, C., van Paradijs, J., Fishman, G. J., Briggs, M. S., Kommers, J., Harmon, B. A., Meegan, C. A., & Lewin, W. H. G. 1996b, Nature, 379, 799
Lamb, D. Q., Miller, M. C., & Taam, R. E. 1996, preprint (astro/ph-9604089)
Lewin, W. H. G., Rutledge, R. E., Kommers, J. M., van Paradijs, J., & Kouveliotou, C. 1996, ApJ, 462, L39
Lewin, W. H. G., van Paradijs, J., & Taam, R. E. 1995, in X-Ray Binaries, ed. W. H. G. Lewin, J. van Paradijs, & E. P. J. van den Heuvel (Cambridge: Cambridge Univ), 196
Paciesas, W. S., et al. 1996, IAU Circ. 6284
Stark, M. J., Ahearn, A. M., Duva, L. J., & Jahoda, K. 1997, preprint (astro/ph-9712154)
Strickman, M. S., et al. 1996, ApJ, 464, L131
van Paradijs, J. 1995, in X-Ray Binaries, ed. W. H. G. Lewin, J. van Paradijs, & E. P. J. van den Heuvel (Cambridge: Cambridge Univ.), 196
Woods, P., Kouveliotou, C., van Paradijs, J., Koshut, T., Finger, M., Fishman, G., & Lewin, W. H. G. 1999, in preparation